Lattice dynamics and anomalous softening in the YbFe_{4}Sb_{12} skutterudite

A. Möchel, I. Sergueev, H.-C. Wille, J. Voigt, M. Prager, M. B. Stone, B. C. Sales, Z. Guguchia, A. Shengelaya, V. Keppens, and R. P. Hermann

Phys. Rev. B **84**, 184306 — Published 29 November 2011

DOI: 10.1103/PhysRevB.84.184306

Lattice dynamics and anomalous softening in the $YbFe_4Sb_{12}$ skutterudite

A. Möchel,[1,2] I. Sergueev,[3] H.-C. Wille,[4] J. Voigt,[1] M. Prager,[1,*] M. B. Stone,[5] B. C. Sales,[6] Z. Guguchia,[7] A. Shengelaya,[7] V. Keppens,[8] and R. P. Hermann[1,2,†]

[1]*Jülich Centre for Neutron Science JCNS and Peter Grünberg Institut PGI, JARA-FIT, Forschungszentrum Jülich GmbH, D-52425 Jülich, Germany*
[2]*Faculté des Sciences, Université de Liège, B-4000 Liège, Belgium*
[3]*European Synchrotron Radiation Facility, F-38043 Grenoble Cedex, France*
[4]*Deutsches Elektronen-Synchrotron, D-22607 Hamburg, Germany*
[5]*Neutron Scattering Sciences Division, Oak Ridge National Laboratory, Oak Ridge, TN 37831, USA*
[6]*Oak Ridge National Laboratory, Oak Ridge, TN 37831-6393, USA*
[7]*Department of Physics, Tbilisi State University, GE-0128 Tbilisi, Georgia*
[8]*Department of Materials Science and Engineering, University of Tennessee, Knoxville, TN 37996, USA*

The lattice dynamics of the filled skutterudite $YbFe_4Sb_{12}$ were studied by resonant ultrasound spectroscopy and an anomalous softening in the temperature dependence of the elastic constants at ∼50 K was observed. This anomaly can not be explained by the dynamics of the filler, in contrast to other filled skutterudites. We have further investigated the origin of this anomaly using macroscopic and microscopic measurements. A rearrangement of the spectral weight of the Yb phonon states was observed in the temperature dependence of the density of phonon states, obtained by inelastic neutron scattering. We suggest that the anomaly is due to a change of the Yb valence state and that the anomaly and the phonon spectral weight rearrangement have the same origin.

PACS numbers: 63.20.D-, 62.20.de, 72.20.Pa, 61.05.C-, 76.30.-v

I. INTRODUCTION

The interest in skutterudites and their lattice dynamics drastically increased in the last two decades due to their potential application in thermoelectric devices[1–6]. Efficient thermoelectric materials are required to have both a good electrical conductivity and a poor thermal conductivity. Filled and unfilled skutterudites are promising candidates for thermoelectric applications at elevated temperatures[1], because they can simultaneously fulfill these two requirements. The thermal conductivity of skutterudites can be tuned by filling[1,2] these cage structure with heavy elements such as La, Ce, Eu, or Yb with only a slight influence on their electrical properties. Macroscopic measurements of filled skutterudites and their unfilled parent compounds have shown that the reduction of thermal conductivity is related to the nature of the filler[3–6]. Different models with various degrees of details were suggested, which aim to explain the low thermal conductivity in filled cage structures such as skutterudites and clathrates: a) The decrease of the thermal conductivity is caused by the dynamics of the guest atom[3,5,7,8]. The phonon modes of these fillers impede the acoustic phonons and for this reason the phonon mean free path and the lattice thermal conductivity are reduced with respect to the unfilled compound. b) An avoided crossing of cage and filler phonon modes takes place. This flattens the phonon modes and therefore the velocity of sound, which is proportional to the thermal conductivity is reduced[9,10]. c) Phonon-phonon Umklapp scattering takes place and the heat transport is hindered[9,11,12]. However, a detailed quantitative understanding of the thermal transport in these systems has not yet been obtained.

For filled skutterudites it was suggested that the low thermal conductivity is due to the dynamics of the fillers, also known as 'rattlers'[3]. In order to investigate the influence of the filler atom on the lattice dynamics, the elastic constants of filled skutterudites, *e.g.*, $La_{0.9}Fe_3CoSb_{12}$, were studied by resonant ultrasound spectroscopy (RUS)[13]. An anomaly, attributed to the localized phonon modes of the fillers, was observed in the temperature dependence of the elastic constants. The elastic response of a two-level system accurately models the observed anomaly[13]. The level spacing is in good agreement with the energy of the localized filler mode observed in the density of phonon states (DPS) measured by inelastic neutron scattering.

The filled skutterudite $YbFe_4Sb_{12}$ exhibits interesting magnetic and electrical properties, which were intensively studied[14–22] in the last 13 years. Due to the low thermal conductivity found in this system[17], it is also an interesting model system to study the role of the filler atoms on the lattice dynamics[12]. The parent compound $FeSb_3$ of RFe_4Sb_{12}, where R denotes the filler atom, was not available until recently[23], therefore the isostructural system $CoSb_3$ has often been taken for comparison of RFe_4Sb_{12} with the unfilled structure[3,24,25]. The unfilled compound $CoSb_3$ exhibits a larger thermal conductivity compared to the thermal conductivity in $YbFe_4Sb_{12}$ and it was assumed as for many other cage systems that the low thermal conductivity in $YbFe_4Sb_{12}$ is solely due to the filler.

The valence state of Yb in $YbFe_4Sb_{12}$ is controversially discussed in the literature. It was first suggested that the Yb valence state is intermediate between Yb^{2+} and Yb^{3+}, because of the magnetic mo-

ment of $\sim$4 μ_B per formula unit, which was obtained by magnetization measurements. This moment is intermediate between $\sim$2.5 $\mu_B/f.u.$, which would correspond to a non-magnetic Yb^{2+} state, where the polyanion $[Fe_4Sb_{12}]$ yields the effective moment of 2.5 $\mu_B/f.u.$, and $\sim$6.3 $\mu_B/f.u.$, which would correspond to a magnetic Yb^{3+} valence state[14–18]. Further, it was observed that the effective mass of the conduction electrons is enhanced at low temperatures indicating that $YbFe_4Sb_{12}$ might be a heavy-fermion system[14,16–18]. Indeed, an intermediate valence states of Yb and a Wilson ratio of $\sim$2.6, were obtained by magnetization and heat capacity measurements. A Yb ion valence fluctuation temperature of $\sim$70 K was obtained by infrared spectroscopy measurements[17]. In the temperature dependence of the electrical conductivity a shoulder was observed around this fluctuation temperature[14]. Photoemission spectroscopy measurements at 15 K favor[26] the existence of divalent and trivalent Yb ions in $YbFe_4Sb_{12}$. In contrast to these observations and conclusions, only divalent Yb ions were found[19,27,28] in $YbFe_4Sb_{12}$, measured by X-ray absorption spectroscopy at room temperature and 100 K. Therefore, it was suggested that the previously observed trivalent Yb ion contribution is due to an impurity phase and that after all $YbFe_4Sb_{12}$ is not a heavy-fermion system[22]. No temperature dependence of the Yb valence state is available so far.

Herein, the temperature dependence of the elastic constants of $YbFe_4Sb_{12}$, measured by RUS, are reported. An anomaly is seen at 50 K, which can not be explained by a two-level system model as was used for $La_{0.9}Fe_3CoSb_{12}$. Different scenarios, which would explain the anomaly, are presented. We examined the temperature dependence of the lattice parameter, the magnetization, the density of phonon states and the valence state of Yb in $YbFe_4Sb_{12}$ in order to identify the origin of this anomaly. Temperature dependent X-ray diffraction, magnetization, inelastic neutron scattering, nuclear inelastic scattering and electron paramagnetic resonance measurements were performed. These measurements suggest that a partial valence change of Yb at $\sim$50 K is the reason for the anomaly seen in the elastic constants. Further, a comparison of the density of phonon states in $YbFe_4Sb_{12}$ with the parent compound $FeSb_3$ is given.

II. EXPERIMENTAL

High-quality polycrystalline $YbFe_4Sb_{12}$ samples were prepared by melting stoichiometric quantities of high-purity elements in carbon-coated, sealed and evacuated silica tubes[3]. The density of these samples is 93% of the theoretical value. Resonant ultrasound spectroscopy[29] measurements have been performed as a function of temperature between 5 and 300 K using a homemade probe that fits in a physical properties measurement system from Quantum Design (QD-PPMS). For the RUS measurements the sample was cut and polished into a rectangular parallelepiped.

Temperature dependent diffraction measurements were carried out at the 6-ID-D high-energy station at the Advanced Photon Source between 10 and 300 K, with the sample cooled in a closed cycle cryostat. The X-ray wavelength was fixed at 0.124269 Å. An area detector was used and the sample-detector distance was 1601.1(1) mm, as determined by a NIST SRM640c Si standard. Silicon powder (Chempur, 99.999%) was mixed with the sample and used as an internal standard. The data were reduced to diffraction patterns using Fit2D[30], and were refined with FULLPROF[31].

Magnetization measurements were carried out using a QD-PPMS with the vibrating sample magnetometer option, VSM, between 9 and 300 K with two different applied magnetic fields of 0.1 and 3 T. A hysteresis measurement was performed at 300 K between -1 and $+1$ T.

Measurements of ^{57}Fe Mössbauer spectra have been carried out between 4.2 and 295 K on a constant-acceleration spectrometer with a 295 K rhodium matrix ^{57}Co source. The spectrometer was calibrated at 295 K with α-Fe powder. In order to guarantee reproducibility, measurements between 4.2 and 70 K have been carried out in three independent experimental runs that gave consistently the same results.

The temperature dependence of the density of phonon states, DPS, was measured between 10 and 300 K by inelastic neutron scattering, INS, at the time-of-flight spectrometer ARCS at the Spallation Neutron Source, with an incident neutron energy of 59.5 meV. The data was evaluated at the phonon creation side of the spectrum. An annular Al cylinder was used as a sample holder for $\sim$10 g $YbFe_4Sb_{12}$ powder. The sample holder was sealed under He atmosphere for a better thermal connection between the sample holder and the sample. An empty sample holder was measured under identical conditions in order to perform a background subtraction from the data. The sensitivity of the detectors was normalized to the scattering from a vanadium standard. The data were reduced using DANSE[32] and visualized using DAVE[33].

Nuclear inelastic scattering, NIS, measurements were carried out with the ^{57}Fe and ^{121}Sb resonances at the European Synchrotron Radiation Facility beamlines ID18 and ID22N, respectively, on a $\sim$10 mg $YbFe_4Sb_{12}$ powder sample with natural abundance of the elements. The experimental technique is described elsewhere[34–36]. The resolution was 0.7 and 1.3 meV FWHM for the ^{57}Fe and ^{121}Sb measurement, respectively, as obtained from the nuclear forward scattering (NFS). Due to a larger multiphonon contribution in the ^{121}Sb measurement compared to the ^{57}Fe measurement, and a therefore less precise DPS extraction, all Sb values have larger error bars. The relative multiphonon contribution, $S_{\mathrm{m-ph}}$, depends on the Lamb-Mössbauer factor, f_{LM}, by $S_{\mathrm{m-ph}} \propto 1 - f_{\mathrm{LM}}$. Due to the typically much faster decrease of the Sb f_{LM} with increasing temperature, Sb measurements have to be carried out at low temperature, therefore the data obtained using the ^{121}Sb resonance were measured at 30

and 100 K. The Fe f_{LM} of these materials only slightly decreases with increasing temperature. The Fe measurement was performed at 300 K and the multiphonon contribution was still small compared to the multiphonon contribution in the Sb measurement at 25 K.

Electron paramagnetic resonance measurements, EPR, were done on a powder sample in an applied field between 0 and 400 mT between 11 and 100 K, at a frequency of 9.5 GHz. The EPR measurements were performed with an X-band BRUKER EMX spectrometer equipped with an Oxford Instruments helium flow cryostat. In order to avoid a signal distortion due to skin effects, the samples were ground and the powder was suspended in epoxy.

III. RESULTS AND DISCUSSION

A. Resonant ultrasound spectroscopy

An isotropic polycrystalline solid has two independent elastic constants, a shear modulus c_{44}, governing transverse waves, and a compressional modulus c_{11}, governing longitudinal waves. The quality factor, q, is inversely proportional to the damping, *i.e.*, the energy dissipation in the sample, and was obtained from the linewidth, Δf, of a resonance peak: $1/q = \Delta f/f$.

The temperature dependence of the elastic constants and $1/q$ in $YbFe_4Sb_{12}$ measured by RUS are shown in Fig. 1. In the absence of thermodynamic irregularities, the temperature dependence of the elastic constants can be described by the empirical Varshni function[37], which gradually increases with decreasing temperature and approaches a constant at the lowest temperature, as shown by the dashed-dotted line in Fig. 1 for c_{11}. Our data show two clear deviations from the Varshni function at ∼50 and ∼190 K, reflected also in the temperature dependence of $1/q$. In this manuscript, we will investigate the origin of the anomaly visible as a rapid drop of the elastic constants at ∼50 K.

Previous studies of other filled skutterudites have revealed similar anomalies in the elastic constants at low temperatures. The drop in the temperature dependence of the elastic constants of these systems was explained adequately by the presence of localized vibrational modes of the filler atoms[13]. These modes have a two-level character, with a spacing between the two levels determined by the frequency of the vibrational modes[13]. By taking into account the elastic response of a two-level system with the filler mode frequency as the level spacing, it was possible to model the temperature dependence of the elastic constants in these systems.

The drop in the temperature dependence of the elastic constants in $YbFe_4Sb_{12}$ could be due to various mechanisms: a) If a structural phase transition takes place, the atom positions change and likewise the atomic bondings, which are related to the elastic constants. b) A magnetic phase transition, *e.g.*, from ferromagnetism to paramagnetism, could also produce a step in the temperature dependence of the elastic constants at the Curie temperature, if magnetoelastic interactions are present. c) A change of the frequency of the filler phonon modes would explain such an anomaly: In $YbFe_4Sb_{12}$ the two-level system model can only explain the temperature dependence of the elastic constants, if the spacing between the two levels and hence the frequency of the filler mode changes with temperature, see inset in Fig. 1 for c_{11}. A change in the frequency of the filler mode as a function of temperature could be observed in the temperature dependence of the density of phonon states. d) A change of the valence state of Yb would also affects the interatomic force constants and the elastic constants.

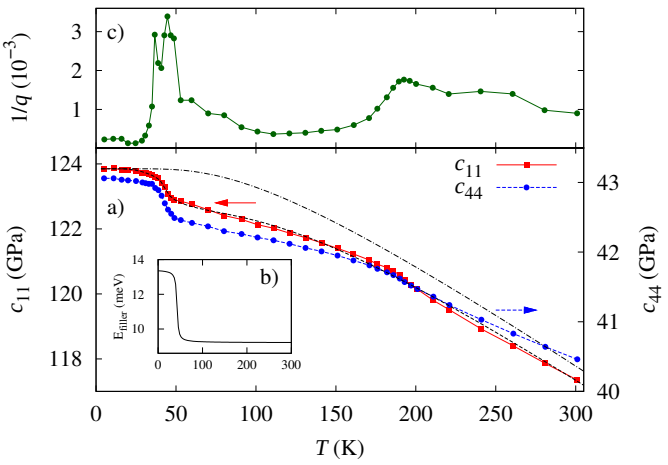

FIG. 1. a) The temperature dependence of the elastic constants c_{11}, left axis, and c_{44}, right axis, of $YbFe_4Sb_{12}$ measured by resonant ultrasound spectroscopy. The dashed-dotted line indicates a Varshni behavior for c_{11}, which would indicate a normal temperature dependence and the dashed line indicates the fit to the data of a two-level system model with a variation of the level spacing with temperature. b) The temperature dependence of the filler mode energy, *i.e.*, the level spacing of the two level system, used for the fit. c) The temperature dependence of the inverse of the quality factor, $1/q$, as described in the text.

In order to investigate if one of the scenarios a)-d) is the origin of this anomaly, the temperature dependence of the lattice parameter, the magnetic susceptibility, the density of phonon states, and the Yb valence state have been investigated by different methods and the findings are reported below.

B. Structure and magnetism

First, we investigate the presence of a possible structural or magnetic phase transition. $YbFe_4Sb_{12}$ exhibits[14] a cubic structure with the space group $Im\bar{3}$. The Yb filler is located in a dodecahedral cage of Sb atoms, also shown in Fig. 2. In the diffraction pattern, not shown, no reflections from a secondary phase were observed. With the

assumption that the Sb site is fully occupied, the composition of $Yb_{0.95(1)}Fe_{3.72(3)}Sb_{12}$ has been obtained from the refinement. The temperature dependence of the lattice parameter and the thermal expansion coefficient, α, are shown in Fig. 3. The lattice parameter obtained by X-ray diffraction refinement, with a Bragg R_B-factor and a R_F-factor of ∼3 and ∼2.5%, respectively, are in good agreement with published X-ray and neutron diffraction data[10,17,19]. In order to reduce noise in the thermal expansion coefficient, especially at low temperatures, the temperature dependence of the lattice parameter, a, was fitted with a third order polynomial function, $a_m(T)$, see fit in Fig. 3. The difference between the modeled $a_m(T)$ and the experimental lattice parameter $a(T)$ is less than 0.0002 Å. The thermal expansion coefficient is then given by $\alpha(T) = (da_m(T)/dT)/a_m(300\ K)$. Within the accuracy of this method, neither a phase transition, nor an anomalous temperature behavior is observed. The anomaly seen in the elastic constants thus seems not related to an anomalous thermal expansion. For comparison the thermal expansion of the unfilled compound[23], $FeSb_3$, is shown in Fig. 3.

The mean-square displacements, $\langle u^2_{eq}\rangle$, are indicative for the movement of an atom. The displacement of Yb is about five times larger than for Sb and shows a different temperature dependence, see Fig. 4. Reliable refinement of the mean-square displacement of Fe was not possible due to the small scattering length compared to Sb and Yb, but the Fe mean-square displacement was obtained from the Fe NIS measurement, see section III E. The filler atom Yb exhibits a localized vibrational mode, see below, and can be assumed to be an Einstein oscillator. From the temperature dependence of the Yb $\langle u^2_{eq}\rangle$ the Einstein temperature, θ_E, can be obtained[38] by $d\langle u^2_{eq}\rangle/dT = \hbar^2/(mk_B\theta^2_E)$ where m is the mass of the atom. The Einstein temperature of 70(5) K was determined in the high temperature approximation from a fit of the Yb $\langle u^2_{eq}\rangle$ between 100 and 300 K, see Fig. 4. The collective modes of the Sb cage can be considered with a Debye model. The Debye temperature, θ_D, can be obtained[38,39] by $d\langle u^2_{eq}\rangle/dT = 3\hbar^2/(mk_B\theta^2_D)$ and the Debye temperature of 240(10) K for Sb has been determined by fitting $\langle u^2_{eq}\rangle^2(T)$ of Sb in the temperature region between 100 and 300 K, see Fig. 4. The value for Sb is in good agreement with the value obtained by the DPS as described below. No anomaly, which could explain the drop in the elastic constants, is observed in the temperature dependence of the $\langle u^2_{eq}\rangle$.

In order to determine whether a magnetic transition could explain the anomalous softening, the temperature dependence of the magnetic susceptibility $\chi = M/H$ with the magnetic moment M and the applied magnetic field $\mu_0 H$ of 0.1 and 3 T was measured. The molar magnetic susceptibility, χ_m, is shown in Fig. 5, after correction of the ferro- and diamagnetic contribution obtained by the hysteresis loop at 300 K, not shown. The data are in good agreement with the data in Ref. [21]. The large increase of the susceptibility below 25 K is a deviation from the

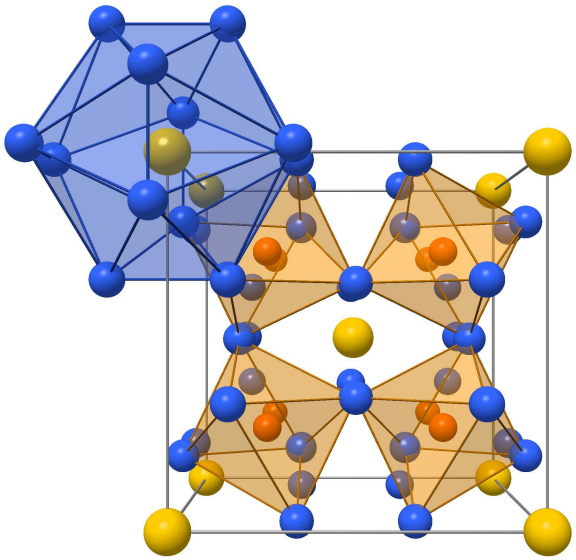

FIG. 2. The crystal structure of $YbFe_4Sb_{12}$. Blue, red and yellow spheres indicate Sb, Fe and Yb, respectively. Yb is located in a Sb dodecahedron (blue shaded) and Fe is located in a Sb octahedron (red shaded).

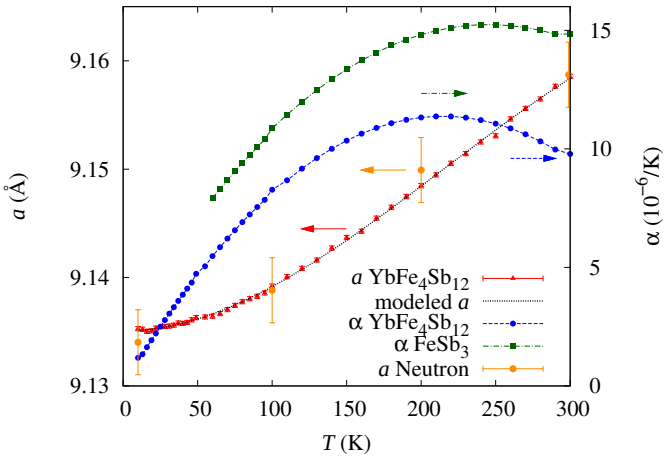

FIG. 3. The temperature dependence of the lattice parameter, a, and the thermal expansion, α, of $YbFe_4Sb_{12}$. For comparison, the thermal expansion of $FeSb_3$ is also shown[23]. The dotted black line indicates the model for the temperature dependence of the lattice parameter a and the dashed lines are extrapolated guides for the eye. The yellow points indicate the lattice parameter determined from the diffraction patterns obtained by integrating over the elastic line in the INS data, see section III D.

paramagnetic behavior and was also observed in other $YbFe_4Sb_{12}$ samples[20,21]. It was suggested that this is due to a magnetic impurity[20]. The inverse susceptibility, see inset to Fig. 5, shows a Curie-Weiss behavior above 100 K. The effective paramagnetic moment of 4.6(2) μ_B per formula unit, obtained by $\mu_{eff} = 797.8\sqrt{\chi_m T}$, is nearly temperature independent above 100 K and is in

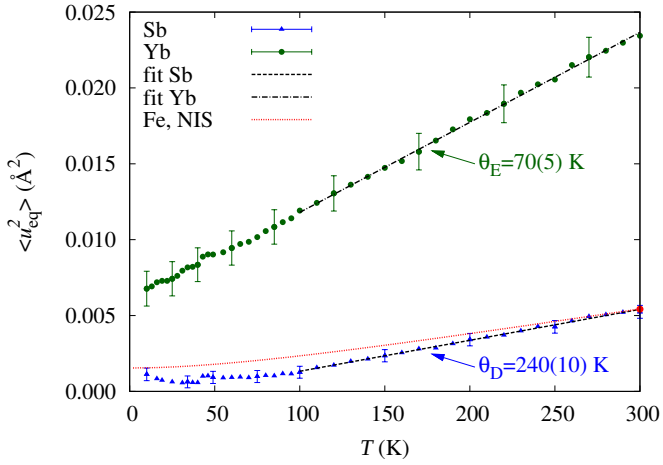

FIG. 4. The temperature dependence of the mean-square displacements of Yb and Sb obtained by X-ray diffraction and the fits between 100 and 300 K for extraction of the Debye and Einstein temperatures, see text. The red line indicates the Fe mean-square displacement obtained from the NIS measurement, see section III E.

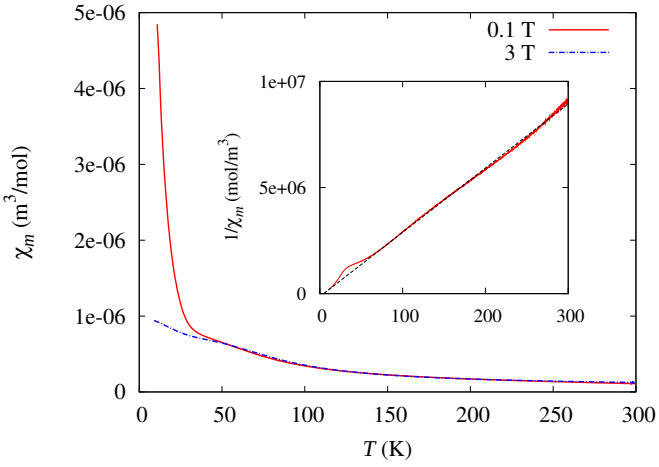

FIG. 5. Magnetic susceptibility of $YbFe_4Sb_{12}$, measured with an applied magnetic field of 0.1 and 3 T. The inset shows the inverse susceptibility and the dashed line represents a linear fit between 100 and 300 K.

fair agreement with literature values[14,15,21], which range from 2.92 to 4.49 $\mu_B/f.u.$. It was discussed[19,21] that the effective magnetic moment is mainly related to the $[Fe_4Sb_{12}]$ polyanion and from impurities in the sample and not from an intrinsic Yb^{3+} contribution.

In order to further assess a possible magnetic origin of the observed anomalous temperature dependence of the elastic constants, RUS measurements were also carried out in an applied field of 0.01 and 3 T and no differences with respect to the measurements without applied field were observed. A magnetic phase transition seems thus unlikely to be the origin of the anomaly seen in the elastic constants.

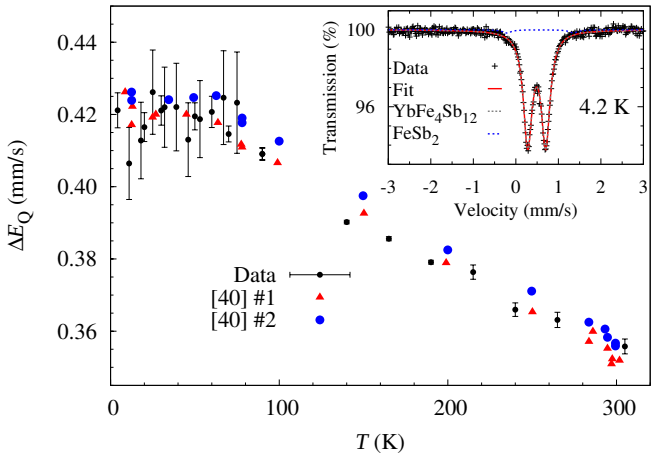

FIG. 6. The quadrupole splitting, ΔE_Q, obtained from the ^{57}Fe Mössbauer spectra. For comparison the data from Ref. [40] are given as red triangles and blue points. The inset shows the Mössbauer spectra at 4.2 K. The blue line indicates the contribution from the $FeSb_2$ impurity.

C. Mössbauer spectroscopy

Temperature dependent Mössbauer spectral measurements were carried out in order to assess both the presence of possible impurities in the sample and whether a visible signature of the step observed in RUS could be detected in the temperature dependence of the isomer shift or quadrupole splitting. The room temperature isomer shift and quadrupole splitting, ΔE_Q, values of 0.380(2) and 0.356(2) mm/s, respectively, are in good agreement with the literature[40]. The linewidth at all temperatures was 0.26-0.28 mm/s, and no attempt to separate contributions attributed to binomial distribution related to partial Yb filling[40] was done. A small impurity of 2.8(1)% of $FeSb_2$ was observed, see inset to Fig. 6, an impurity easily identified by the large ΔE_Q=1.57 mm/s at 4.2 K [41]. As this impurity is not seen in X-ray diffraction it likely consists of small amorphous inclusions. No other impurities are observed. The temperature evolution of the isomer shift, not shown, and the quadrupole splitting, see Fig. 6, are normal without any measurable anomaly around 50 K, in agreement with Tamura et al. [40]. It thus appears that the local environment of Fe is not measurably affected by the anomalous softening observed in RUS.

D. Inelastic neutron scattering

The temperature dependence of the density of phonon states was obtained by inelastic neutron scattering measurements, in order to assess whether there is an energy shift of the phonon modes associated with the filler. The scattering vector, Q, and energy, E, dependent scattering function, $S(Q, E)$, at 10 K is shown in Fig. 7. The scat-

tering intensity exhibits a Q^2 dependence as expected from the inelastic neutron scattering cross section for phonon scattering[42]. Neutron diffraction patterns were obtained by integrating over the elastic line in the INS measurements and as an example the diffraction patterns at 10, 100 and 300 K are shown in Fig. 8. A simulated neutron diffraction pattern calculated by FULLPROF using the 10 K lattice parameter determined by X-ray diffraction, and the Al sample holder scattering are also given for comparison in Fig. 8. The lattice parameter were obtained from these diffraction patterns with a Le Bail fit using FULLPROF and the values are in good agreement with the values obtained by X-ray diffraction, see Fig. 3.

The temperature dependence of the total neutron cross-section weighted DPS was extracted from the inelastic neutron scattering measurements by subtraction of the elastic scattering and the empty can background measurement, and by taking into account the thermal population of the phonon states with the Bose factor[42], see Fig. 7. The DPS area was normalized to one for all temperatures. The multiphonon contribution has been estimated and found to be negligible.

The DPS at 300 K is in good agreement with the published[10,12] DPS measured by INS at 300 K. The peak at 5 meV shifts to higher energies by less than 0.4 meV with increasing temperature. The energy of this peak is in good agreement with the Einstein temperature of 70 K $\approx$ 6 meV, determined from the temperature dependence of the Yb mean square displacements and can thus be attributed to the dynamics of Yb, see also below. The small shift of this peak can not explain the temperature dependence of the Yb phonon mode frequency used for the two-level model. Therefore, a change in energy of the filler mode energy is not a fitting explanation for the anomaly seen in the elastic constants. The small downshift of the high energy phonon modes above $\sim$25 meV, which are mainly related to Fe, see below, is due to the thermal expansion.

Closer inspection reveals a decrease of the peak height at 5 meV in the DPS with increasing temperature, accompanied by an increase of the density of the states between 7 and 12 meV. As discussed below, the states between 7 and 12 meV are mainly related to the dynamics of Sb, see below in the nuclear inelastic scattering data, but also in part to the filler[10,43]. The temperature dependence of the peak areas is shown in the upper panels of Fig. 7. Above $\sim$50 K the area of the 5 meV peak increases and then decreases at $\sim$100 K, while an increase in intensity is observed around $\sim$11 meV. The origin of the temperature dependence of the DPS is not clear, but a rearrangement of the spectral weight of the Yb states obviously takes place. This rearrangement and the drop in the elastic constants likely have the same origin.

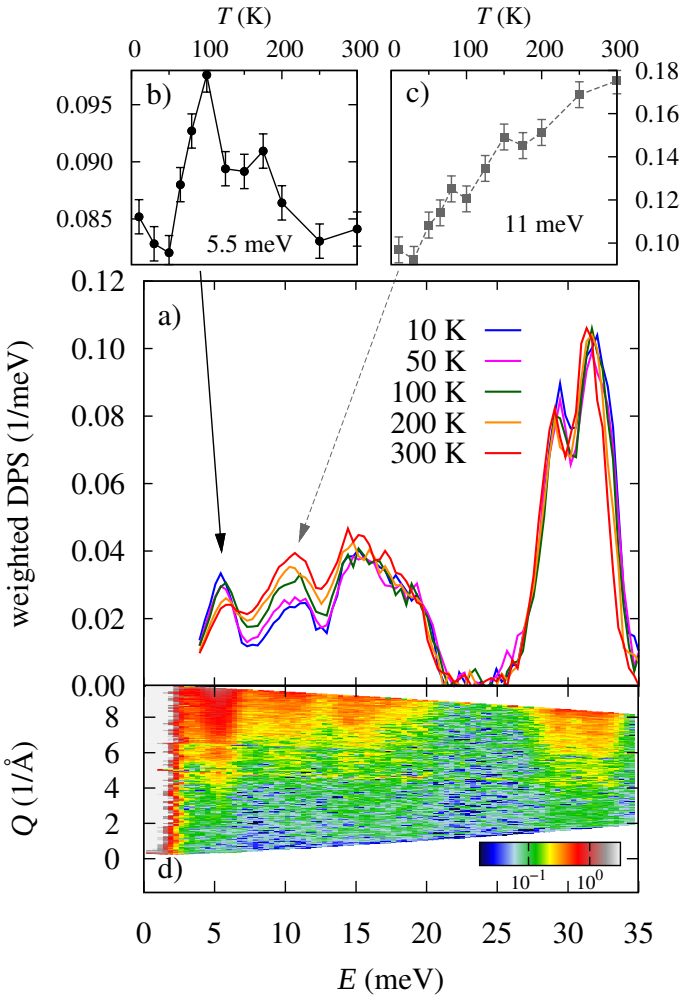

FIG. 7. a) The temperature dependence of the neutron cross section weighted DPS in $YbFe_4Sb_{12}$. The upper panels show the change of the peak area with temperature for the peak at 5.5 meV, b), and for the peak at 11 meV, c). d) The inelastic structure factor $S(Q, E)$ of $YbFe_4Sb_{12}$ measured at 10 K. The colorbox indicates the $S(Q, E)$ intensity.

E. Nuclear inelastic scattering

In order to attribute the phonon modes to specific elements, the partial element specific DPS can be obtained from nuclear inelastic scattering measurements, as this technique is isotope specific. The measurements on $YbFe_4Sb_{12}$ were done in order to get the full partial DPS by combining NIS and INS measurement results. The NIS spectra measured with the ^{57}Fe and ^{121}Sb resonance at 300 and 30 K, respectively, in $YbFe_4Sb_{12}$ are shown in Fig. 9, together with the instrumental resolution function measured by the nuclear forward scattering. The extraction procedure of the DPS from the NIS measurement is explained in Ref. [44] and the comparison of the partial ^{57}Fe and ^{121}Sb DPS, $g(E)$, of $FeSb_3$ from Ref. [23] is shown in Fig. 10. The main Fe modes are two sharp peaks above $\sim$25 meV. The splitting of

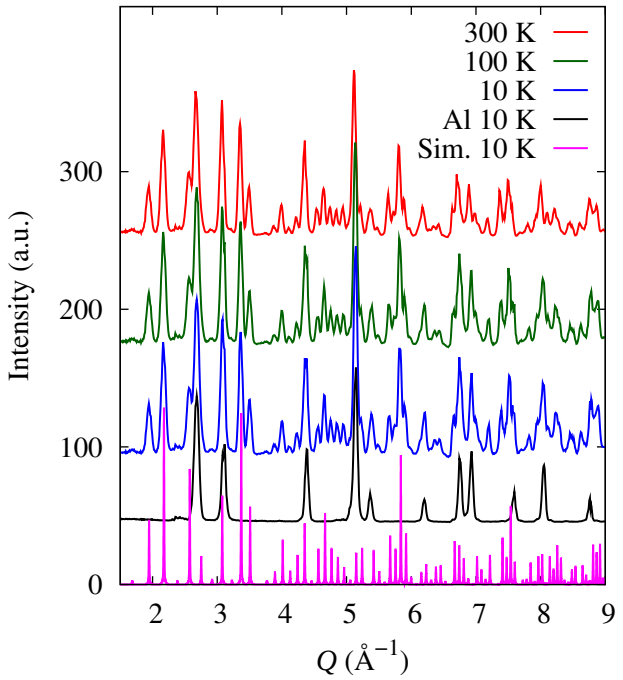

FIG. 8. The neutron diffraction pattern of $YbFe_4Sb_{12}$ and from the Al sample holder obtained from the elastic line in the INS measurements. The data were integrated between 2 and −2 meV energy transfer. The simulated neutron diffraction pattern calculated with FULLPROF with the lattice parameter at 10 K, obtained from X-ray diffraction, is shown as the pink line at the bottom of the figure. The Al diffraction pattern of the background measurement at 10 K is indicated by the black line and was not subtracted from the $YbFe_4Sb_{12}$ pattern shown here.

the peaks was also seen by inelastic neutron scattering measurements[25] in the filled compounds, whereas in the parent compounds $FeSb_3$ [23] and $CoSb_3$ [25] the peaks are not clearly separated. The states are slightly shifted to lower energies in the filled compound compared to the parent compound, which is indicative of a lower mean force constant for Fe in $YbFe_4Sb_{12}$. There is also a small contribution in the Fe DPS between 5 and 20 meV, which corresponds to hybrid Fe and Sb vibrational modes. Similar small contributions are seen in the Sb DPS above ∼25 meV, but the Sb modes are mainly observed below ∼25 meV. In $FeSb_3$ the Sb phonon modes are broader than in $YbFe_4Sb_{12}$.

From the partial DPS, $g(E)$, several lattice dynamics and thermodynamic properties can be directly obtained. For comparison the values for the unfilled compound $FeSb_3$ from Ref. [23] are given. From the low energy limit of the reduced DPS, $g(E)/E^2$, the velocity of sound, v_s, can be obtained by $\lim_{E\to 0}(g(E)/E^2) = m_R/(2\pi^2\rho\hbar^3 v_s^3)$, with the mass of the resonant nucleus, m_R, and the density ρ. The Debye level is indicated in the insets to Fig. 10. From the Fe Debye level of $YbFe_4Sb_{12}$ a velocity of sound of 2600(20) m/s was obtained. For $FeSb_3$ a v_s of 2390(10) m/s was found[23]. These values are in reasonable agreement with the values obtained from the Sb Debye levels, see Table I. The element specific mean force constant, F^m can be determined[34] by $F^m = m_R/\hbar \int_0^\infty g(E)E^2dE$. The Sb F^m is larger in $YbFe_4Sb_{12}$ than in $FeSb_3$, 120(5) and 105(5) N/m, respectively, whereas the Fe F^m is slightly smaller in $YbFe_4Sb_{12}$ than in $FeSb_3$, 182(1) N/m and 186(1) N/m, respectively. The Debye temperature, θ_D, can be obtained by $\theta_D^2 = 3/(k_B{}^2 \int_0^\infty g(E)dE/E^2)$ in the high temperature limit, see Ref. [34], with k_B the Boltzman constant. For $YbFe_4Sb_{12}$ Debye temperatures of 230(10) and 285(5) K were found for Sb and Fe, respectively, whereas for $FeSb_3$ 210(10) and 370(5) K were obtained for the Sb and Fe Debye temperature, respectively. The atomic mean-square displacement can be calculated from the Lamb-Mössbauer factor, f_{LM}, obtained from the NIS measurement, by $\langle u_{eq}^2\rangle = -\ln(f_{LM})/k^2$, where k is the incident wavevector[34]. The mean-square displacement of Fe at 300 K is shown in Fig. 4 as a dot. The temperature dependence of the Fe mean-square displacement was calculated in the harmonic approximation[34] and is indicated by a line.

TABLE I. Summary of the thermodynamic properties obtained by the partial DPS for $YbFe_4Sb_{12}$ and $FeSb_3$.

	$YbFe_4Sb_{12}$		$FeSb_3$ from Ref. [23]	
	Sb	Fe	Sb	Fe
v_s (m/s)	2400(100)	2600(20)	2400(100)	2390(10)
F^m (N/m)	120(5)	182(1)	105(5)	186(1)
θ_D (K)	230(10)	385(5)	210(10)	370(5)

A summary of the thermodynamic properties is given in Table I. Summarizing, the binding of Fe is slightly decreased, whereas the Sb binding is increased by filling the structure. $FeSb_3$ is thus slightly softer than $YbFe_4Sb_{12}$, which is evidence that the lowering of the thermal conductivity in filled RFe_4Sb_{12} skutterudites compared to $CoSb_3$ is partly due to the softer $[Fe_4Sb_{12}]$ framework and the influence of the filler on the thermal conductivity should be revisited, see Ref. [45].

Combining the NIS and INS measurement, the full partial DPS can be evaluated, see Fig. 11. The Sb and Fe partial DPS are weighted by the neutron cross sections and $YbFe_4Sb_{12}$ stoichiometry. From this comparison it is clear that the phonon modes below 7 meV are related to Yb. NIS measurements were also done at 100 K with the ^{121}Sb resonance, see inset to Fig. 11. Due to the even higher multiphonon contribution, the DPS can not be extracted as accurately as at low temperatures. There is a small energy shift towards lower values in the antimony DPS with increasing temperature. This indicates a normal temperature dependent behavior due to the thermal expansion and elastic softening. Except for this energy shift, there is no other temperature dependence of the DPS. In summary from inelastic scattering we have to

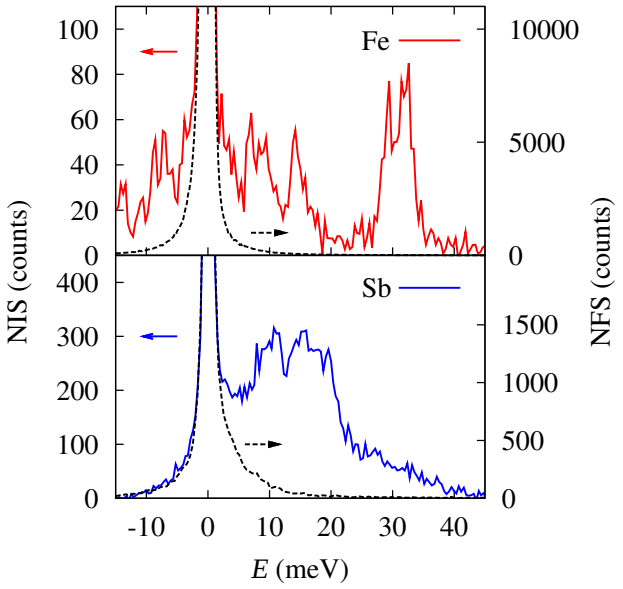

FIG. 9. The NIS and nuclear forward scattering, NFS, measured at the ^{57}Fe, top, and ^{121}Sb, bottom, resonances on $YbFe_4Sb_{12}$. The black lines indicate the nuclear forward scattering.

conclude that the rearrangement of the spectral weight in the DPS at low energies is mainly due to a change in the dynamics of Yb and does not measurably affect Sb or Fe.

F. Valence state

In order to obtain information about the Yb valence state, temperature dependent EPR measurements were performed and are shown in Fig. 12. A broad signal in low magnetic fields can be ascribed to ferromagnetic impurities based on the temperature dependence of the signal intensity. The presence of ferromagnetic impurities was also confirmed by magnetization measurements, see section III B. Below 50 K another signal with the g-factor $g \approx 4.17$ appears in the EPR spectra and its intensity increases with decreasing temperature as can be seen in Fig. 12. Since Yb^{2+} ions have fully occupied 4f states, they can not provide an EPR signal and from Mössbauer measurements we obtained that the Fe valence state is not changing with temperature. Therefore we assume that this signal is due to Yb^{3+} ions. This would indicate a change of the valence state of a part of the Yb^{2+} ions to Yb^{3+} ions below 50 K. As Yb is only a second nearest neighbor of Fe, it thus is not surprising that a partial valence change of Yb would not measurably affect the Fe Mössbauer spectra as discussed above. Obviously, a valence change will modify the bonding of Yb with its nearest neighbors and therefore influence the lattice dynamics. We conclude that the partial valence change is the most likely origin of the anomaly seen in the temperature dependence of the elastic constants and the DPS. A suitable model for the temperature dependence of the elastic constants, which takes a partial valence change into account, could not be derived so far.

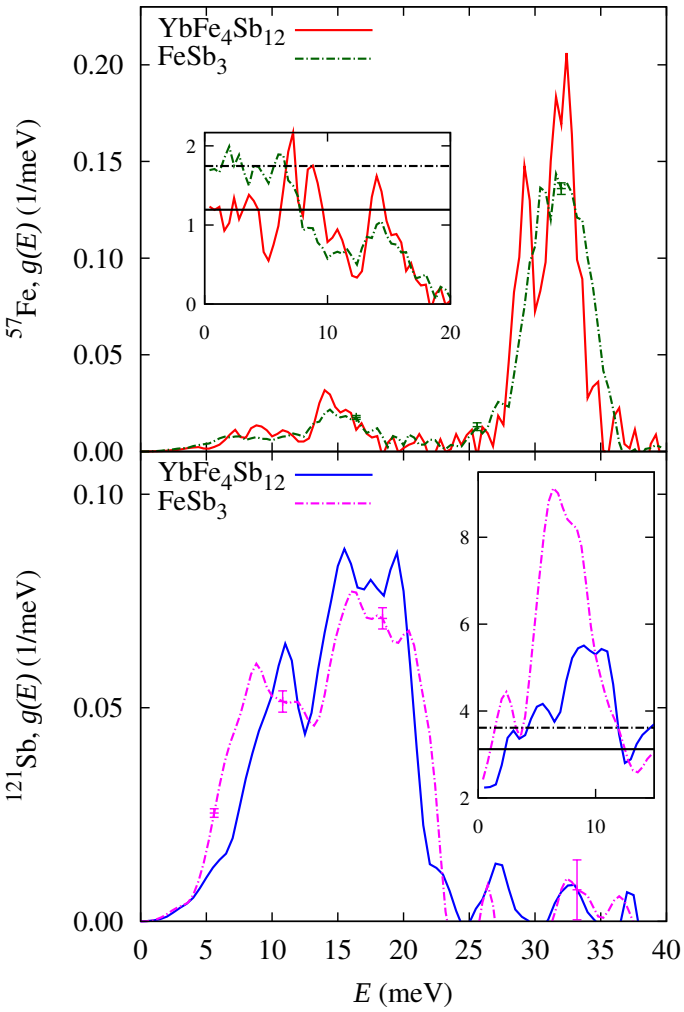

FIG. 10. The partial DPS of $YbFe_4Sb_{12}$ of ^{57}Fe, top, and ^{121}Sb, bottom, in comparison to the partial DPS of $FeSb_3$ from Ref. [23]. The insets show the reduced DPS, $g(E)/E^2$, and the Debye levels, black lines in the same line style, obtained at low energies.

The valence state of Yb could also be directly obtained by X-ray photoemission and X-ray absorption spectroscopy. With these methods, different $YbFe_4Sb_{12}$ samples were studied in Ref. [19, 26, and 28] at various temperatures, but we could not find studies reporting both room temperature and low temperature measurements. Measurements at room temperature and 100 K were carried out in Ref. [19] and [28], respectively. The observed large signal of Yb^{2+} and the quite weak signal of Yb^{3+}, was related to impurities in the sample. In Ref. [26] the measurement was carried out at 10 K and the authors conclude that the major Yb signal indicates Yb^{2+}, and no indication of the presence of Yb^{3+} was found. The contradictory results of these studies can

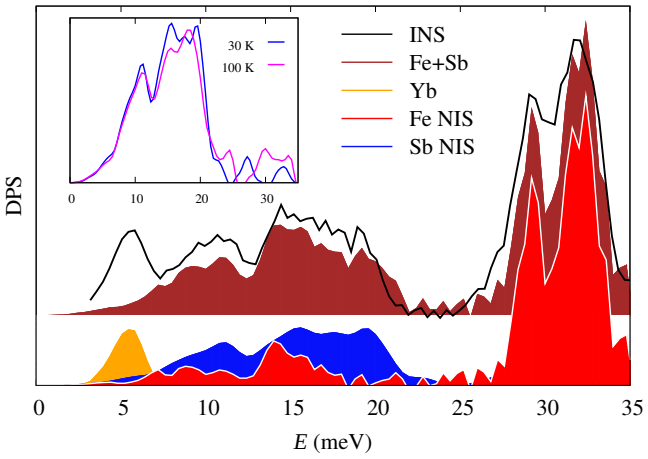

FIG. 11. Comparison between the DPS of $YbFe_4Sb_{12}$ obtained by INS at 65 K, black line, and the DPS obtained by NIS with the ^{121}Sb resonance, blue, and with the ^{57}Fe resonance, red. The NIS data are normalized to the neutron scattering cross section and the stoichiometry of the sample. The orange area indicates the Yb DPS obtained by subtraction of the Sb and Fe DPS from the total DPS obtained by INS. The brown area indicates the added normalized DPS from Sb and Fe obtained by NIS. The inset shows the temperature dependence of the Sb DPS obtained by NIS.

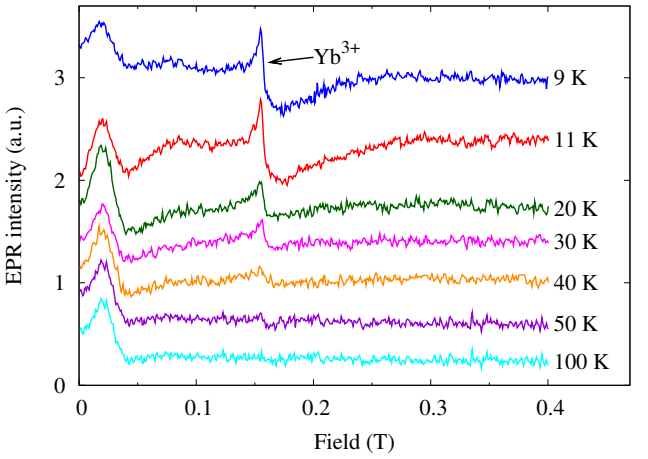

FIG. 12. Temperature dependent EPR measurements on $YbFe_4Sb_{12}$ with an applied frequency of 9.5 GHz. The signal arising below 50 K is most likely due to Yb^{3+} ions.

also be explained by a partial valence change of Yb with temperature. Both results are in agreement with our temperature dependent EPR measurements. In order to clarify the temperature dependence of the valence state of Yb as suggested above, the valence state of Yb should be measured directly by X-ray photoemission or X-ray absorption spectroscopy in further experiments, both above and below ∼50 K.

IV. CONCLUSION

An anomalous softening of the elastic constants of $YbFe_4Sb_{12}$ was observed at ∼50 K. This anomaly can not be explained by the dynamics of the filler atom, as in the filled skutterudite[13] $La_{0.9}Fe_3CoSb_{12}$. Measurements of the lattice parameter and the susceptibility do not provide any evidence for a structural or magnetic phase transition that could explain the anomaly. X-ray diffraction and magnetization measurements reveal that the sample is single phase with a very small amount of magnetic impurities. A rearrangement of the Yb density of phonon states is observed in the temperature dependence of the DPS, however, our results do not show any continuous shift of the Yb phonon modes, which would be sufficient to explain the anomalous softening. In the EPR measurements an additional signal has been observed below 50 K and we suggest that this signal is due to a change of the Yb valence state. The anomaly in the temperature dependence of the elastic constants is thus very likely linked to the change of the Yb valence state. Furthermore, the comparison of the partial DPS of $YbFe_4Sb_{12}$ and $FeSb_3$ reveals, that the lattice dynamics of the $[Fe_4Sb_{12}]$ framework does only slightly change upon filling the structure.

ACKNOWLEDGMENTS

We thank Dr. D. Robinson and Mr. D. Bessas for their support during the synchrotron radiation measurements and Prof. H. Schober and Dr. M. M. Koza for helpful discussions. We thank Prof. F. Grandjean and Dr. L. Rebbouh for their help during the Mössbauer spectral measurements. The European Synchrotron Radiation Facility, the Advanced Photon Source and the Spallation Neutron Source are acknowledged for provision of synchrotron and neutron beam time at the nuclear resonance station ID18 and ID22N, the high energy station 6-ID-D and the wide Angular-Range Chopper Spectrometer, respectively. RH acknowledges support from the Helmholtz-University Young Investigator Group 'Lattices Dynamics in Emerging Functional Materials'. A portion of this Research at Oak Ridge National Laboratory's Spallation Neutron Source was sponsored by the Scientific User Facilities Division, Office of Basic Energy Sciences, U. S. Department of Energy.

* deceased
† r.hermann@fz-juelich.de

[1] B. C. Sales, D. Mandrus, and R. K. Williams, Science **272**, 1325-1328 (1996).

[2] G. S. Nolas, D. T. Morelli, and T. M. Tritt, Annu. Rev. Mater. Sci. **29**, 89-116 (1999).

[3] B. C. Sales, D. Mandrus, B. C. Chakoumakos, V. Keppens, and J. R. Thompson, Phys. Rev. B **56**, 15081-15089 (1997).

[4] D. T. Morelli, G. P. Meisner, B. X. Chen, S. Q. Hu, and C. Uher, Phys. Rev. B **56**, 7376-7383 (1997).

[5] G. S. Nolas, J. L. Cohn, and G. A. Slack, Phys. Rev. B **58**, 164-170 (1998).

[6] G. S. Nolas, M. Kaeser, R. T. Littleton, and T. M. Tritt, Appl. Phys. Lett. **77**, 1855-1857 (2000).

[7] B. C. Sales, B. C. Chakoumakos, and D. Mandrus, Phys. Rev. B **61**, 2475-2481 (2000).

[8] G. J. Long, R. P. Hermann, F. Grandjean, E. E. Alp, W. Sturhahn, C. E. Johnson, D. E. Brown, O. Leupold, and R. Rüffer, Phys. Rev. B **71**, 140302 (2005).

[9] M. Christensen, A. B. Abrahamsen, N. B. Christensen, F. Juranyi, N. H. Andersen, K. Lefmann, J. Andreasson, C. R. H. Bahl, and B. B. Iversen, Nature Materials **7**, 811-815 (2008).

[10] M. M. Koza, L. Capogna, A. Leithe-Jasper, H. Rosner, W. Schnelle, H. Mutka, M. R. Johnson, C. Ritter, and Y. Grin, Phys. Rev. B **81**, 174302 (2010).

[11] M. M. Koza, M. R. Johnson, R. Viennois, H. Mutka, L. Girard, and D. Ravot, Nature Materials **7**, 805-810 (2008).

[12] M. M. Koza, A. Leithe-Jasper, H. Rosner, W. Schnelle, H. Mutka, M. R. Johnson, M. Krisch, L. Capogna, and Y. Grin, Phys. Rev. B **84**, 014306 (2011).

[13] V. Keppens, D. Mandrus, B. C. Sales, B. C. Chakoumakos P. Dai, R. Coldea, M. B. Maple, D. A. Gajewski, E. J. Freeman, and S. Bennington, Nature **395**, 876-878 (1998).

[14] N. R. Dilley, E. J. Freeman, E. D. Bauer, and M. B. Maple, Phys. Rev. B **58**, 6287-6290 (1998).

[15] A. Leithe-Jasper, D. Kaczorowski, P. Rogl, J. Bogner, M. Reissner, W. Steiner, G. Wiesinger, and C. Godart, Solid State Commun. **109**, 395-400 (1999).

[16] M. B. Maple, N. R. Dilley, D. A. Gajewski, E. D. Bauer, E. J. Freeman, R. Chau, D. Mandrus, and B. C. Sales, Physica B **259-261**, 8-9 (1999).

[17] N. R. Dilley, E. D. Bauer, M. B. Maple, S. Dordevic, D. N. Basov, F. Freibert, T. W. Darling, A. Migliori, B. C. Chakoumakos, and B. C. Sales, Phys. Rev. B **61**, 4608-4614 (2000).

[18] E. D. Bauer, R. Chau, N. R. Dilley, M. B. Maple, D. Mandrus, and B. C. Sales, J. Phys.: Condens. Matter **12**, 1261-1267 (2000).

[19] W. Schnelle, A. Leithe-Jasper, M. Schmidt, H. Rosner, H. Borrmann, U. Burkhardt, J. A. Mydosh, and Y. Grin, Phys. Rev. B **72**, 020402 (2005).

[20] E. Alleno, D. Berardan, C. Godart, and P. Bonville, Physica B: Condensed Matter **378-380**, 237-238 (2006).

[21] T. Ikeno, A. Mitsuda, T. Mizushima, T. Kuwai, Y. Isikawa, and I. Tamura, JPSJ **76**, 024708 (2007).

[22] W. Schnelle, A. Leithe-Jasper, H. Rosner, R. Cardoso-Gil, R. Gumeniuk, D. Trots, J. A. Mydosh, and Y. Grin, Phys. Rev. B **77**, 094421 (2008).

[23] A. Möchel, I. Sergueev, N. Nguyen, G. J. Long, F. Grandjean, D. C. Johnson, and R. P. Hermann, Phys. Rev. B **84**, 064302 (2011).

[24] G. P. Meisner, D. T. Morelli, S. Q. Hu, J. Yang, and C. Uher, Phys. Rev. Lett. **80**, 3551-3554 (1998).

[25] J. L. Feldman, P. Dai, T. Enck, B. C. Sales, D. Mandrus, and D. J. Singh, Phys. Rev. B **73**, 014306 (2006).

[26] T. Okane, S. Fujimori, K. Mamiya, J. Okamoto, Y. Muramatsu, A. Fujimori, Y. Nagamoto, and T. Koyanagi, J. Phys.: Condens. Matter **15**, 2197-2200 (2003).

[27] D. Berardan, C. Godart, E. Alleno, S. Berger, and E. Bauer, J. Alloys Compd. **351**, 18-23 (2003).

[28] Y. S. Dedkov, S. L. Molodtsov, H. Rosner, A. Leithe-Jasper, W. Schnelle, M. Schmidt, and Y. Grin, Physica C **460**, 698-699 (2007)

[29] A. Migliori, J. L. Sarrao, W. M. Visscher, T. M. Bell, M. Lei, Z. Fisk, and R. G. Leisure, PHYSICA B **183**, 1-24 (1993), and A. Migliori, and J.L. Sarrao, *Resonant ultrasound spectroscopy* (Wiley, New York, 1997).

[30] A. P. Hammersley, *ESRF Internal Report*, **ESRF97HA02T**, 'FIT2D: An Introduction and Overview', (1997).

[31] J. Rodriguez-Carvajal, *FULLPROF V (2009)* (Laboratoire Leon Brillouin (CEA-CNRS), France, 2009).

[32] *http://docs.danse.us/DrChops*.

[33] R. T. Azuah, L. R. Kneller, Y. M. Qiu, P. L. W. Tregenna-Piggott, C. M. Brown, J. R. D. Copley, and R. M. Dimeo, J. Res. Natl. Inst. Stan. Technol. **114**, 341 (2009).

[34] R. Rüffer, and A. I. Chumakov, Hyp. Interact. **128**, 255-272 (2000).

[35] I. Sergueev, H.-C. Wille, R. P. Hermann, D. Bessas, Y. V. Shvyd'ko, M. Zajac, and R. Rüffer, J. Synchrotron Rad. **18**, 802-810 (2011).

[36] H.-C. Wille, R. P. Hermann, I. Sergueev, O. Leupold, P. van der Linden, B. C. Sales, F. Grandjean, G. J. Long, R. Rüffer, and Y. V. Shvyd'ko, Phys. Rev. B **76**, 140301(R) (2007).

[37] Y. P. Varshni, Phys. Rev. B **2**, 3952-3958 (1970).

[38] B. C. Sales, B. C. Chakoumakos, D. Mandrus, J. W. Sharp, N. R. Dilley, and M. B. Maple, Materials Research Society symposia proceedings **545**, 13-21 (1999).

[39] B. T. M. Willis and A. W. Pryor, *Thermal Vibrations in Crystallography* (Cambridge University Press, 1975).

[40] I. Tamura, T. Ikeno, T. Mizushima, and Y. Isikawa, JPSJ **75**, 014707 (2006).

[41] R. Hu, R. P. Hermann, F. Grandjean, Y. Lee, J. B. Warren, V. F. Mitrovic, and C. Petrovic, Phys. Rev. B **76**, 224422 (2007).

[42] G. L. Squires, *Introduction to the theory of thermal neutron scattering*, (Cambridge University Press, 1978).

[43] J. L. Feldman, D. J. Singh, C. Kendziora, D. Mandrus, and B. C. Sales, Phys. Rev. B **68**, 094301 (2003).

[44] W. Sturhahn, T. S. Toellner, E. E. Alp, X. Zhang, M. Ando, Y. Yoda, S. Kikuta, M. Seto, C. W. Kimball, and B. Dabrowski, Phys. Rev. Lett. **74**, 3832-3835 (1995).

[45] M. Christensen, N. Lock, J. Overgaard, and B. B. Iversen, J. Am. Chem. Soc. **128**, 15657-15665 (2006).